Conformational Flexibility of Aqueous Monomeric and Dimeric Insulin: A Molecular Dynamics Study†

Alan E. Mark,*,‡ Herman J. C. Berendsen,§ and Wilfred F. van Gunsteren‡

Laboratorium für Physikalische Chemie, ETH-Zentrum, CH-8092 Zürich, Switzerland, and Laboratory for Physical Chemistry, University of Groningen, Nijenborgh 16, 9747 AG Groningen, The Netherlands

Received May 21, 1991; Revised Manuscript Received August 27, 1991

ABSTRACT: A series of molecular dynamics simulations have been used to investigate the nature of monomeric and dimeric insulin in aqueous solution. It is shown that in the absence of crystal contacts both monomeric and dimeric insulin have a high degree of intrinsic flexibility. Neither of the two monomer conformations of 2Zn crystalline insulin appears to be favored in solution nor is the asymmetry of the crystal dimer reduced in the absence of crystal contacts. A shift is observed in the relative positions of molecules 1 and 2 in the dimer compared with that found in the crystal, which may have consequences for the prediction of the effects of mutants in the monomer–monomer interface designed to alter the self-association properties of insulin.

The current image of the structure of insulin is one primarily based on X-ray crystallographic data, as despite intensive study over many decades comparatively little is known in regard to the solution structure of the most probable active form of the hormone, the monomer. This is primarily because native insulin, close to physiological pH and at concentrations normally required for physicochemical studies, strongly self-associates in solution to form a complex mixture of polymeric species. In particular this has thus far prevented detailed structural analysis using high-resolution NMR, although some progress has recently been made using native insulin under extreme solvent conditions (Kline & Justice, 1990) and using mutant insulins with altered association properties (Boelens et al., 1990; Kristensen et al., 1991).

Insulin crystallizes in a variety of different forms suitable for X-ray diffraction. Only in the case of despentapeptide insulin, however, is the basic unit the monomer (Bi et al., 1984; Liang et al., 1985). In all other cases insulin crystallizes as a dimer or higher aggregate, often with different conformations for the different molecules in the asymmetric unit. Detailed analysis of and comparison between the various crystal forms has led to an image of insulin as a molecule in which the major part of the atomic arrangement is relatively rigid and common among a variety of crystal forms (Baker et al., 1988, Chothia et al., 1983). The conformational variations that are observed have been largely attributed to crystal packing forces. In the case of 2Zn insulin it has been proposed that structural differences between the two monomers, which together form the basic asymmetric unit, the dimer, originate from contacts at the hexamer interface. These contacts are said to preferentially deform molecule 2 (Chinese nomenclature) and result in a rotation of the N-terminal segment of the A chain by 33° about ϕ of residue A6. This in turn forces the rotation of Tyr A19 and the displacement Phe B25 relative to molecule 1 (Chothia et al., 1983). In contrast, molecule 1, in light of its close similarity to several other crystalline forms, is viewed as having the preferred conformation, a conformation which is probably similar if not identical to that in solution. There is, however, evidence from binding studies using modified insulins suggesting that this is not the form of the hormone that interacts with the receptor and that a conformational change occurs before or during binding to the receptor (Dodson et al., 1983). Furthermore changes in the ^{1}H NMR spectrum and circular dichroism spectrum of native insulin at high dilution indicate that there are conformational differences between the monomeric and aggregated forms (Pocker & Biswas 1980; Roy et al., 1990).

Two previous simulation studies have addressed the question of the structure of the insulin monomer in the absence of crystal contacts. Wodak et al. (1984) demonstrated that energy minimization of the isolated molecules could remove the main differences between molecules 1 and 2 in 2Zn insulin. Energy minimization using steepest descent or conjugate gradient methods can basically only find the closest minimum, traveling always downhill over the potential energy surface. In an attempt to identify alternative stable conformations and to assess the range of the available conformational space, Krüger et al. (1987) conducted independent molecular dynamics (MD) simulations of each molecule in vacuo. In the absence of solvent, root mean square (RMS) fluctuations of all atoms are reduced. In particular, the motions of exposed side chains can be significantly affected. The stability of internal hydrogen-bond networks can also be increased as alternate interactions with water are not possible. It is not surprising, therefore, that little variation from the starting crystal structure was observed.

The present study attempts to further define the nature of noncrystalline insulin. We have independently simulated molecule 1 and molecule 2 of 2Zn insulin in aqueous solution with full atomic charges and counter ions each for a total time of 100 ps. In addition, a dimer, the so called OP dimer (Blundell et al., 1972), again in the presence of water and counter ions, was also simulated for 100 ps under similar conditions. The simulation of the dimer is of interest not only for comparison to the monomer but also because of the continuing interest in the nature of the self-interaction itself. Mutant forms of insulin with altered aggregation properties have potential in slow- or fast-acting therapeutic formulations (Brange et al., 1988). On the basis of close contacts in the monomer–monomer interface found in the crystal, a number of residues have been substituted. The effect of individual substitutions varies greatly and highlights the need for a better understanding of the interactions driving the association process.

† This work was supported by the Netherlands Foundation for Chemical Research (SON) with financial aid from the Netherlands Organization for Scientific Research (NWO).

* To whom correspondence should be addressed.

‡ ETH-Zentrum.

§ University of Groningen.

0006-2960/91/0430-10866$02.50/0

Table I: Box Type and Parameters

system	box type	X (nm)	Y (nm)	Z (nm)	waters	atoms total
monomer 1	truncated octahedron	4.90	4.90	4.90	1708	5616
monomer 2	truncated octahedron	4.80	4.80	4.80	1604	5304
dimer	rectangular	3.79	4.64	5.73	2849	9531

Over the last few years a number of small proteins have been studied by MD simulation involving aqueous solution using periodic boundary conditions: bovine pancreatic trypsin inhibitor (van Gunsteren & Berendsen, 1984; Ghosh & McCammon, 1987; Levitt & Sharon, 1988), avian pancreatic polypeptide (Krüger et al., 1985), parvalbumin (Ahlström et al., 1987), calbindin D_{9k} (Ahlström et al., 1989), the third domain of silver pheasant ovomucoid (Jorgensen & Tirado-Rives, 1989), and barnase (Van Belle et al., 1989). These studies concern a single simulation of a single protein molecule. Only three studies of complex formation in aqueous solution with periodic boundary conditions have been published: Wong and McCammon (1986a,b) studied a trypsin–benzamidine complex, de Vlieg et al. (1989) simulated the lac repressor headpiece complexed with its 14 base pair DNA operator, and Harte et al. (1990) examined the HIV-1 protease dimer. Our present study of insulin involves protein–protein complex formation. It differs from the protein simulations mentioned above by a comparison between the complexed and uncomplexed states. In addition, a comparison of MD trajectories starting from different initial structures is made.

Materials and Methods

The initial atomic coordinates used for each of the three simulations, monomer 1, monomer 2, and the OP dimer, were taken from the X-ray structure of rhombohedral 2Zn porcine insulin, entry 1ins of the Brookhaven Protein Data Bank (Bernstein et al., 1977; Blundell et al., 1972). The coordinates of polar hydrogens were generated from standard geometries and were treated explicitly throughout the simulations. Nonpolar hydrogens were treated by way of the united atom approach. The GROMOS force field was used for the simulations (van Gunsteren & Berendsen, 1987).

After the generation of the polar hydrogens, each structure was subjected to an initial 100 steps of steepest descent energy minimization (EM) in vacuo to relax strain in the X-ray structures. Solvent was then introduced by placing each molecule in the center of either a truncated octahedron in the case of the monomer or a rectangular box in the case of the dimer. The dimensions of the respective boxes were chosen such that the minimum distance of any protein atom to the wall of the box was 0.65 nm. Water molecules were inserted into each box by immersion in an equilibrium configuration of bulk SPC (Berendsen et al., 1981) water and subsequently removing all water molecules that are outside the box or of which the oxygen atom lies within 0.23 nm of a non-hydrogen protein atom. The actual box sizes and the number of water molecules introduced in each system are given in Table I. In order to relax strong nonbonded interactions generated between the water and the protein and between individual water molecules during this process, 100 steps of steepest descent EM was performed while keeping the protein atoms positionally restrained to their initial positions using an harmonic potential with a force constant of $K = 9000$ kJ mol^{-1} nm^{-2}.

The overall charge of insulin per monomer is −2.0 at pH 7.0. In order neutralize the overall system and to ensure an effective ionic strength of 0.1, a total of three Na^+ and one Cl^- ions were added per monomer to each system as follows. The electrical potential was calculated at all water oxygen positions, and the water molecule at the lowest or highest potential replaced with a Na^+ or Cl^- ion accordingly unless this water lies within 0.35 nm of a non-hydrogen protein atom or another ion. This process was repeated until all ions were added. This again was followed by 50 steps of EM of the entire system in order to relax unfavorable short-range ion–water interactions.

Initial velocities for the atoms were taken from a Maxwellian distribution at 300 K. The protein and the water were independently weakly coupled to a temperature bath of $T = 300$ K with a relaxation time of 0.1 ps for an initial period of 10 ps before the temperature of the bath was increased to $T = 350$ K (Berendsen et al., 1984). The higher temperature was chosen in order to facilitate the crossing of potential energy barriers and to obtain a fuller impression of the range of available configurational space in the limited simulation time available. In addition to running the simulation at 350 K and after an initial 50 ps of simulation, the masses of all atoms in the system involving the dimer were set to 1.0 amu. This was done in order to further facilitate the sampling of configurational space. It should be noted that although dynamical information is lost, equilibrium properties of the system such as the average conformation, hydrogen-bonding properties, and positional fluctuations are independent of the mass of each atom (Bennett, 1975).

Each simulation was run at constant volume using periodic boundary conditions and an integration time step of $t = 2$ fs. Bond lengths were constrained to equilibrium values using the SHAKE algorithm (Ryckaert et al., 1977; van Gunsteren & Berendsen, 1977). Nonbonded interactions were evaluated using a twin range method. Short-range interactions were evaluated each time step using a 0.8-nm cutoff radius. Longer range Coulombic interactions were evaluated every 10th time step and held constant for the intervening steps. The long-range cutoff radii were 1.2 and 1.5 nm for the monomer and dimer simulations, respectively. Cutoff radii were applied to the centers of geometry of neutral atom groups (charge groups) and to the oxygen atoms of the water. As the potential energy is dominated by electrostatic terms, the long-range cutoffs were chosen as large as practical while maintaining the minimum image convention. This implies, however, that a few atoms at the extremities of the molecule are capable of interacting with a few protein atoms in the next periodic image. This may have enforced unwanted periodicity on the system.

On the basis of the total potential energy of the system, initial equilibration was seen to have been achieved within 20 ps. Analysis was thus performed using transient structures written at intervals of 0.05 ps from 30 to 100 ps in the case of the two monomers and between 50 and 100 ps in the case of the dimer. Both the simulations and analysis were carried out using programs contained in the GROMOS[1] library (van Gunsteren & Berendsen, 1987).

Results and Discussion

General Comments. In contrast to the results of Krüger et al. (1987) which showed significant convergence of the two structures within 120 ps in vacuo, we observe that (overall) the structures continually diverge both from each other and from their respective starting structures during the course of

[1] The GROMOS (Groningen molecular simulation) program library which was used to perform the simulations presented is available from BIOMOS b.v., Laboratory of Physical Chemistry, ETH-Zentrum, CH-8092 Zürich, Switzerland, at nominal cost.

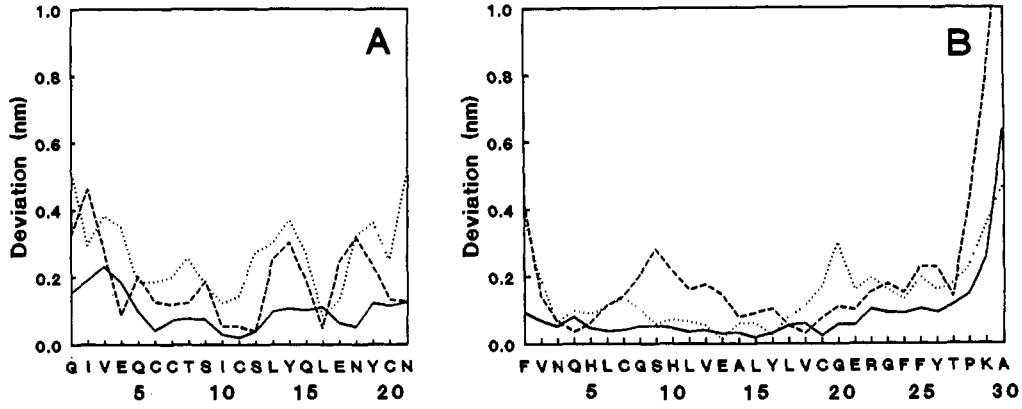

FIGURE 1: Positional deviations between α-carbons in molecules 1 and 2 after optimal fitting of all α-carbons as a function of residue number (left, A chain; right, B chain). (---) Average over 30-100ps for monomeric insulin, (···) average over 50–100 ps for dimeric insulin, and (—) the X-ray structure.

Table II: RMS Deviations between α-Carbons (Upper Right) and All Atoms (Lower Left) for the X-ray and the Average of the Simulated Structures after Optimal Fit on All α-Carbons[a]

		structure					
		X-ray		monomer		dimer	
	molecule	1	2	1	2	1	2
X-ray	1		0.118	0.160	0.212	0.123	0.212
	2	0.211		0.214	0.158	0.163	0.220
monomer	1	0.275	0.298		0.285	0.120	0.244
	2	0.292	0.236	0.334		0.240	0.251
dimer	1	0.255	0.266	0.189	0.286		0.234
	2	0.304	0.298	0.331	0.307	0.316	

[a] Averages were taken over all transient structures from 30 to 100 ps and from 50 to 100 ps for monomeric and dimeric insulin, respectively. Deviations are expressed in nanometers.

Table III: Contributions to the Total Potential Energy of Interactions Involving the Protein Averaged over 80–100 ps for Monomeric Molecules 1 and 2, Together with RMS fluctuations

	monomer 1 (kJ/mol)	monomer 2 (kJ/mol)
bond angle	873 ± 45	864 ± 46
improper dihedral	290 ± 24	290 ± 25
dihedral	322 ± 24	321 ± 28
internal electric	−2347 ± 100	−2363 ± 175
internal LJ[a]	−1166 ± 40	−1171 ± 38
electric protein–ions	−541 ± 110	−534 ± 103
LJ[a] protein–ions	<1	<1
electric protein–water	−6234 ± 201	−6288 ± 239
LJ[a] protein–water	−1216 ± 68	−1115 ± 70
total	−10015 ± 217	−9997 ± 209

[a] Lennard-Jones.

the 100-ps simulations. Table II shows the root mean square (RMS) deviations between the starting X-ray structures and the averages of the simulations for monomer and dimeric molecules 1 and 2. The largest deviation is seen between the averages of the two structures simulated as monomers. Neither of the two crystal forms appears to be favored in the monomer. Both structures remain closer to their initial conformation than to the initial conformation of the other. In the dimer there is also significantly greater deviation between the averages of the simulation than the averages compared to their respective starting configurations. Molecule 2 in the dimer shows the greatest differences to all other molecules. In contrast, molecule 1 in the dimer remains close to the starting configuration. It is also very close to the average of monomeric molecule 1, which indicates that both simulations have explored similar regions of configurational space. This may possibly indicate a higher degree of stability for the molecule 1 conformation, but it would be unwise to attribute much significance to this result.

Although the two insulin molecules simulated as monomers show significant structural differences, energetically they are equivalent. Table III shows a breakdown of the components of the total potential energy for interactions involving the protein for each of the two monomers averaged over the final 20 ps (80–100 ps) of the simulation. Not only is the total potential energy almost equal but each of the components are roughly equivalent. As expected, the electrostatic interactions between the water and the protein dominate. This underlines the importance of the inclusion of water in the simulation. At the start of the simulation the interaction between water and the protein was 500 kJ/mol more favorable in the case of molecule 2 than for molecule 1. During the initial 20-ps equilibration time, the value of molecule 1 rapidly approached that of molecule 2.

Comparison between Molecules 1 and 2. Deviations between the C_α carbons, after least-squares fitting over all C_α atoms, in the averaged structures of molecules 1 and 2 as a function of amino acid residue for the monomer (---) and the dimer (···) are shown in Figure 1. The solid line in Figure 1 shows the deviations observed experimentally in the crystal. As previously indicated in Table II, it can seen from Figure 1 that deviations between the average structures of molecules 1 and 2 simulated as the monomer and dimer in solution are significantly larger than observed experimentally in the crystal. The largest overall deviations occur in the A chain and the carboxy terminus of the B chain. The large deviations between C_α atoms in the A chains, especially in the dimer, tend against the hypothesis of a single preferred conformation which is distorted in the crystal due to packing forces. The A chain appears to be capable of large-scale motions pinned by cystine residues involved in disulfide bridges (A6–A11, A7–B7, and A20–B19) and by Leu A16, which lies fully buried close to the center of the molecule (Baker et al., 1988). Deviations between C_α atoms in the region B8–B16 are significantly smaller in the dimer than as monomers. Residues B8, B9, B12, B13, and B16 are all involved in forming close contacts in the monomer–monomer interface (Blundell et al., 1972). This is also reflected in the magnitude of the RMS fluctuations of the C_α atoms shown in Figure 2. In the region B8–B19, the fluctuations in the dimer are reduced compared with that found in the monomer and reflect an increase in the stability of the B9–B19 α-helix, which is largely buried in the dimer. This is consistent with results from circular dichroism studies which indicate less helix content in monomeric as compared to polymeric insulin (Pocker & Biswas, 1980; Melberg &

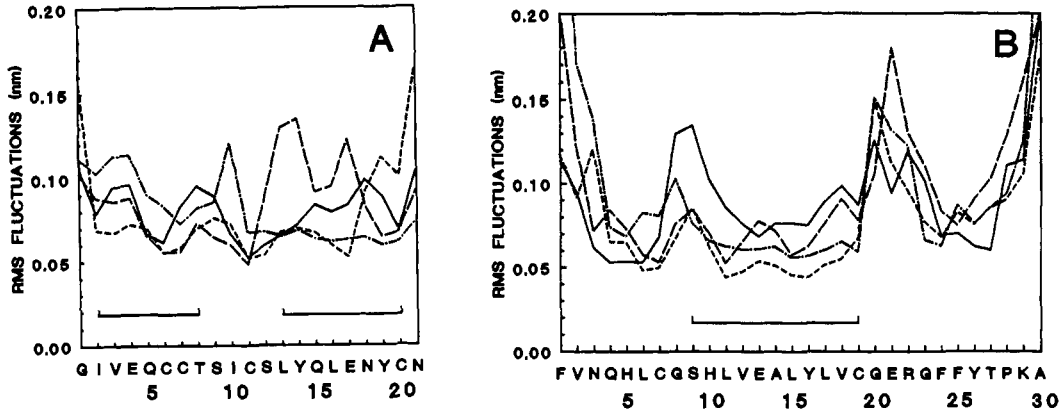

FIGURE 2: Root mean square positional fluctuations of α-carbons as a function of residue number (left, A chain; right, B chain). Fluctuations were determined from the trajectory after best fitting each transient structure on all α-carbons. Fluctuations are shown for monomeric molecules 1 (---) and 2 (—) and dimeric molecules 1 (-·-) and 2 (---). Helical segments in the crystal structure are indicated by the solid bars.

Table IV: Intrachain Hydrogen Bonds Formed as a Percentage of Total Simulation Time (>10%) between the Backbone Atoms in the A Chain for Monomeric Molecule 1 and Molecule 2 and Dimeric Molecule 1 and Molecule 2 (Chinese Nomenclature)

type	donor			acceptor			monomer mol 1	monomer mol 2	dimer mol 1	dimer mol 2	X-ray mol 1	X-ray mol 2
α	A5	Gln	N	A1	Gly	O	86	87	62		*	*
α	A6	Cys	N	A2	Ile	O	30	91	76	92	*	*
3_{10}	A6	Cys	N	A3	Val	O	18		16			
α	A7	Cys	N	A3	Val	O	84	38	64	45	*	
3_{10}	A7	Cys	N	A4	Glu	O				19		
π	A8	Thr	N	A3	Val	O	17		15		*	
α	A8	Thr	N	A4	Glu	O	16	36	32	71		*
3_{10}	A8	Thr	N	A5	Gln	O		23		13		
π	A9	Ser	N	A4	Glu	O	62		76		*	
α	A9	Ser	N	A5	Gln	O		79		81		*
3_{10}	A15	Gln	N	A12	Ser	O	13	11				
α	A16	Leu	N	A12	Ser	O	88	80	74	95	*	*
α	A17	Glu	N	A13	Leu	O	84	90	93	91		*
α	A18	Asn	N	A14	Tyr	O	36	51	84	91		
3_{10}	A18	Asn	N	A15	Gln	O	46	16			*	*
α	A19	Tyr	N	A15	Gln	O	22	30	33	69		
3_{10}	A19	Tyr	N	A16	Leu	O	23	36	48	17	*	*
	A19	Tyr	N	A17	Glu	O		16				
α	A20	Cys	N	A16	Leu	O			11			
3_{10}	A20	Cys	N	A17	Glu	O	29		57		*	*
	A20	Cys	N	A18	Asn	O		28				

Johnson, 1990). Residues B7–B10 in monomeric molecule 2 move through an arc of 0.35 nm during the course of the simulation. With the exception of the N- and C-termini the largest fluctuations are observed in Glu B21 and Arg B22, which are flanked by two glycine residues B20 and B23. The residues form the center of a 1–4 turn and project out into the solvent. It is evident from the differences in the RMS fluctuations between the molecules that the system is far from equilibrium. A substantial amount of the initial character of the starting structure has been maintained. An example of this can be seen in the higher fluctuations of B1 and B2 in molecule 1 as compared with molecule 2 in both the monomer and dimer. For this reason the apparent preservation of the main features of the crystal structure in the monomer may simply be a reflection of a long structural relation time with respect to the simulation time available.

Intramolecular Hydrogen Bonds. Although there is no explicit hydrogen-bonding term in the GROMOS force field, the effect of hydrogen bonds is mimicked by a combination of Lennard-Jones and electrostatic terms. This has been shown to be very effective in the prediction of hydrogen-bonding patterns. A hydrogen bond is considered to exist if the proton–acceptor distance does not exceed 0.25 nm and the donor–proton–acceptor angle is larger then 135°. The hydrogen bonds formed between backbone atoms in the A chain are given in Table IV. Hydrogen bonds were calculated at every time frame of the stored trajectory and are expressed as the percentage of the total simulation time that they were found to exist. Only hydrogen bonds that existed for more than 10% of the total time were considered significant. Overall the basic hydrogen-bonding pattern found in the crystal is maintained in the simulation. The π-helix-type character of the interaction Thr A8–Val A3 and Ser A9–Glu A4 is as in the crystal and in contrast to the vacuum simulation of Krüger et al. (1987), only observed in molecule 1. The helix A16 to A20 does, however, adopt a more regular $[(i + 4) - i]$ structure than observed in the crystal, the interaction A18–A14 being preferred to the A18–A15 interaction especially in the dimer. This was also observed in the simulation of crystalline despentapeptide insulin (Shi Yun-yu et al., 1988). One effect of the addition of solvent has been to destabilize the helix A1–A9. The stability of hydrogen bonds is reduced as compared to vacuum simulations. No interaction between A5 and A1 in molecule 2 of the dimer was observed. The vacant sites are taken up by interactions with water. Hydrogen bonds from Cys A20 to the backbone are also absent. This is reflected in the increased RMS fluctuations of both ends of the A chain in this molecule.

The hydrogen-bonding pattern between backbone atoms in the B chain (Table V) indicates in general a regularization

Table V: Intrachain Hydrogen Bonds Formed as a Percentage of Total Simulation Time (>10%) between the Backbone Atoms of the B Chain for Monomeric Molecule 1 and Molecule 2 and Dimeric Molecule 1 and Molecule 2 (Chinese Nomenclature)

type	donor			acceptor			monomer mol 1	monomer mol 2	dimer mol 1	dimer mol 2	X-ray mol 1	X-ray mol 2
3_{10}	B10	His	N	B7	Cys	O		35		16		
α	B11	Leu	N	B7	Cys	O	78	28	74	73		
3_{10}	B11	Leu	N	B8	Gly	O		24			*	*
α	B12	Val	N	B8	Gly	O	78	16	71	88		
α	B13	Glu	N	B9	Ser	O	75	46	85	63	*	*
α	B14	Ala	N	B10	His	O	91	63	95	83	*	*
α	B15	Leu	N	B11	Leu	O	96	92	97	99	*	*
α	B16	Tyr	N	B12	Val	O	82	89	91	93	*	*
α	B17	Leu	N	B13	Glu	O	78	76	84	69	*	*
3_{10}	B17	Leu	N	B14	Ala	O				11		
α	B18	Val	N	B14	Ala	O	84	85	84	75	*	*
3_{10}	B18	Val	N	B15	Leu	O			11	11		
α	B19	Cys	N	B15	Leu	O	89	81	93	79	*	*
π	B20	Gly	N	B15	Leu	O				26		
α	B20	Gly	N	B16	Tyr	O	50	19	10		*	*
3_{10}	B20	Gly	N	B17	Leu	O		11	10			
3_{10}	B22	Arg	N	B19	Cys	O	38	17	16	13	*	*
α	B23	Gly	N	B19	Cys	O		24	27	62		
3_{10}	B23	Gly	N	B20	Gly	O		14		19	*	*
3_{10}	B30	Ala	N	B27	Thr	O					*	

Table VI: Hydrogen Bonds Formed as a Percentage of Total Simulation Time (>10%) between the A and B Chains for Monomeric Molecule 1 and Molecule 2 and Dimeric Molecule 1 and Molecule 2 (Chinese Nomenclature)

donor			acceptor			monomer mol 1	monomer mol 2	dimer mol 1	dimer mol 2	X-ray mol 1	X-ray mol 2
A2	Ile	N	B27	Thr	O	25					
A11	Cys	N	B4	Gln	O	68	92	51	79	*	*
A13	Leu	N	B2	Val	O		64				
A13	Leu	N	B4	Gln	OE1				16		
A21	Asn	N	B23	Gly	O	85	40	88	11	*	*
A21	Asn	ND2	B22	Arg	O			66			
B3	Asn	ND2	A10	Ile	O	21			34		
B4	Gln	N	A11	Cys	O	68	92	24	56	*	*
B5	His	ND1	A6	Cys	O	18	47	47			
B5	His	ND1	A9	Ser	O		19	10			
B6	Leu	N	A6	Cys	O	50	40	24	54	*	*
B25	Phe	N	A19	Tyr	O	28	60	59		*	*
B25	Phe	N	A20	Cys	O		14				
B25	Phe	N	A21	Asn	OD1	26		10	31		
B27	Thr	OG1	A4	Glu	OE1		24				
B29	Lys	N	A4	Glu	OE2				45		
B29	Lys	N	A4	Glu	OE1				33		*
B30	Ala	N	A4	Glu	OE1				11		

of the helix toward α-type pairing during the simulation. This is associated with an extension of the helix toward the N-terminus. Some 3_{10} character is retained by residues B7–B12 in monomeric molecule 2. This reflects the high mobility of this segment which adopts a number of conformations during the simulation of this molecule. The C-terminal region of the helix (B20–B23) shows a wide variety of hydrogen-bonding patterns, again corresponding with high flexibility.

Hydrogen bonds between the A and the B chains of each molecule are given in Table VI. The observed bonding pattern is different for each molecule. This is further indication that in fact each molecule is exploring a different region of conformational space during the simulation. The lifetimes of the individual hydrogen bonds have important implications in regard to the time that would be required for the system to converge. Two apparently stable hydrogen bonds, one from Leu A13 to Val B2 in monomeric molecule 2 and the other from Asn A21 to Arg B22 in molecule 1 in the dimer, both of which exist for more than 60% of the total simulation time, were not observed for more than 5% in any of the other molecules.

The Dimer and Stabilization of the Monomer–Monomer Interface. During the course of the simulation of the dimer, a shift in the relative position of molecule 2 in relation to molecule 1 compared to the relative position in the crystal was observed. This shift is illustrated in Figure 3, which shows a superposition of the X-ray structure (filled lines) and the trajectory average from 50–100 ps of the simulation (unfilled lines). For clarity only C_α atoms are shown. The molecules are rotated so as to attain a best fit over all C_α atoms in molecule 1. The observed shift appears primarily to be associated with a rotation of approximately 8° about an axis roughly coincident with the backbone of residues B24–B26 in molecule 2. This straightening of the molecule is most probably related to the absence of the Zn ions. The average shift of C_α atoms in the B chain helix is on the order of 0.2 nm. This shift does not appear to significantly disrupt close contacts in the monomer–monomer interface. In Figure 4 nonbonded contacts within 0.4 nm are schematically represented. When Figure 4 is compared to the equivalent figure (fig 6.4) of Baker et al. (1988), it can be seen that the majority of contacts observed in the crystal are maintained during the simulation. Additional contacts were observed between Val B12 and Phe B24 and between Arg B22 of molecule 1 and Pro B28 of molecule 2. No close contacts involving Lys B29 were seen. Contacts to Gly B20, Glu B21, and Asn A21 were reduced.

Direct hydrogen bonds between molecule 1 and molecule

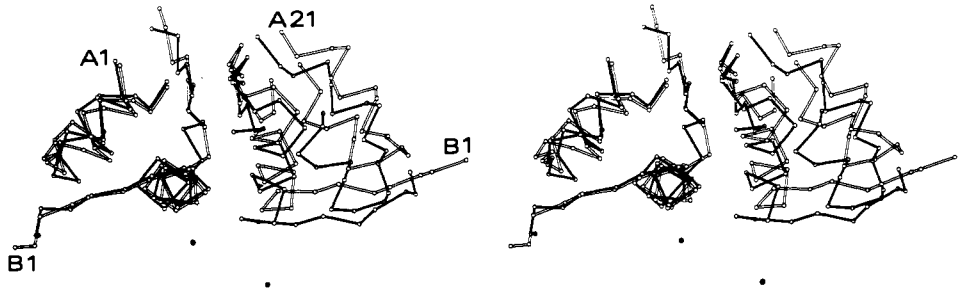

FIGURE 3: Superposition of the C_α backbone of the X-ray (filled) and the trajectory average 50–100 ps (unfilled) of the insulin dimer after a best fit rotation of all C_α atoms of molecule 1. The positions of the two Zn ions in the crystal structure are indicated by the solid spheres.

Table VII: Hydrogen Bonds Found as a Percentage of Total Simulation Time (>10%) between Molecules 1 and 2 (Chinese Nomenclature) in the Dimer

donor				acceptor				percent	X-ray
1	A21	Asn	ND2	2	B26	Tyr	O	21	
1	B24	Phe	N	2	B26	Tyr	O	64	*
1	B26	Tyr	N	2	B24	Phe	O	71	*
2	B24	Phe	N	1	B26	Tyr	O	83	*
2	B26	Tyr	N	1	B24	Phe	O	71	*

2 are listed in Table VII. In addition to bonds between the backbone atoms of Phe B24 and Tyr B26 which form a short segment of antiparallel β-sheet seen in the crystal, an additional hydrogen bond from the side chain of Asn A21 in molecule 1 to the backbone oxygen of Tyr B26 in molecule 2 existed for 21% of the simulation time. The interaction from B24 in molecule 1 to B26 in molecule 2 was reduced by a comparable amount. In addition to direct hydrogen bonds, a number of water-mediated hydrogen bonds were evident between residues in molecule 1 and residues in molecule 2. These interactions may also contribute to the overall stability of the dimer in solution. The most stable of these interactions were between the backbone oxygen of Tyr B16 in both molecules and the phenolic oxygen of Tyr B26 of the other. Water molecules also were observed bridging the two Glu B13 residues.

In conclusion, we can state that this work has demonstrated that both monomeric and dimeric insulin can exhibit a high degree of conformational flexibility in aqueous solution. In particular, it has been demonstrated that in the absence of crystal contacts neither the structure of molecule 1 or molecule 2 in 2Zn crystalline insulin appears to be favored significantly. Differences in hydrogen-bonding patterns and RMS fluctuations of individual atoms indicate that each of the four molecules explored different regions of conformational space. The different regions of configurational space appear, however, to be energetically equivalent. No convergence of the individual structures was observed during the 100 ps of simulation. Furthermore, the lifetimes of individual hydrogen bonds indicate that significant convergence is unlikely to occur within a 200- or even 300-ps simulation.

This finding casts a shadow over the possibility of computing the relative free energy of association of insulin mutants, since this type of calculation only yields reliable free energies when the systems that are considered (1) are in equilibrium and (2) the equilibrium states are sufficiently sampled. Our insulin simulations indicate that simulations far beyond 100 ps would be required to meet these conditions. If such a calculation was to be tried, it would be necessary to repeat the calculation starting from different initial conditions in order to obtain an indication of the dependence the computed free energy of the initial conditions.

The simulation of the dimer has indicated that in solution the position of monomer 2 is shifted relative to monomer 1.

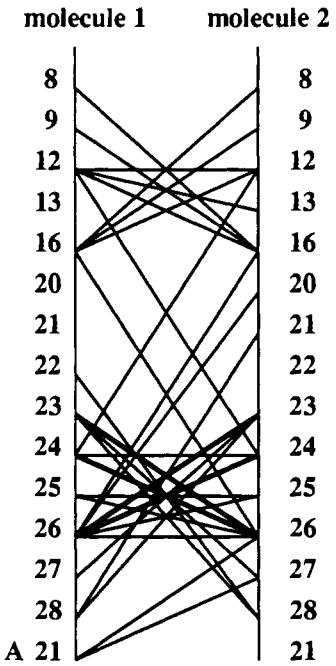

FIGURE 4: Schematic view of nonbonded contacts between residues within the dimer. Lines represent distances ≤0.4 nm. Thick lines represent distances ≤0.35 nm. Distances were determined as trajectory averages from 50 to 100 ps between the centers of heavy atoms.

This shift corresponds to a straightening of the dimer and may be related to the reduced propensity of insulin to form hexamers in the absence of divalent cations.

Registry No. Insulin, 9004-10-8; Zn insulin, 8049-62-5.

REFERENCES

Ahlström, P., Teleman, O., Jönsson, B., & Forsén, S. (1987) *J. Am. Chem. Soc. 109*, 1541–1551.

Ahlström, P., Teleman, O., Kördel, J., Forsén, S., & Jönsson, B. (1989) *Biochemistry 28*, 3205–3211.

Baker, E. N., Blundell, T. L., Cutfield, J. F., Cutfield, S. M., Dodson, E. J., Dodson, G. G., Hodgkin, D. C., Hubbard, R. E., Isaacs, N. W., Reynolds, C. D., Sakabe, K., Sakabe, N., & Vijayan, N. M. (1988) *Phil. Trans. R. Soc. London B319*, 369–456.

Bennett, C. H. (1975) *J. Comput. Phys. 19*, 267.

Berendsen, H. J. C., Postma, J. P. M., van Gunsteren, W. F., & Hermans, J. (1981) in *Intermolecular Forces* (Pullman, B., Ed.) pp 331–342 Reidel, Dordrecht.

Berendsen, H. J. C., Postma, J. P. M., van Gunsteren, W. F., DiNola, A., & Haak, J. R. (1984) *J. Chem. Phys. 81*, 3684–3690.

Bernstein, F. C., Koetzle, T. F., Williams, G. B., Meyer, G. F., Price, M. D., Rodgers, J. R., Kennard, O., Shimanouchi, T., & Tasumi, M. (1977) *J. Mol. Biol. 122*, 535–542.

Bi, R. C., Dauter, Z., Dodson, E., Dodson, G., Giordano, F., & Reynolds, C. (1984) *Biopolymers 23*, 391–395.
Blundell, T., Dodson, G., Hodgkin, D., & Mercola, D. (1972) *Adv. Protein Chem. 26*, 279–402.
Boelens, R., Ganadu, M. L., Verheyden, P., & Kaptein, R. (1990) *Eur. J. Biochem. 191*, 147–153.
Brange, J., Ribel, U., Hansen, J. F., Dodson, G. G., Hansen, M. T., Havelund, S., Melberg, S. G., Norris, F., Norris, K., Snel, L., Sorensen, A. R., & Voigt, H. O. (1988) *Nature 333*, 679–682.
Chothia, C., Lesk, A. M., Dodson, G. G., & Hodgkin, D. C. (1983) *Nature 302*, 500–505.
de Vlieg, J., Berendsen, H. J. C., & van Gunsteren, W. F. (1989) *Proteins 6*, 104–127.
Dodson, E. J., Dodson, G. G., Hubbard, R. E., & Reynolds, C. D. (1983) *Biopolymers 22*, 281–291.
Ghosh, I., & McCammon, J. A. (1987) *J. Phys. Chem. 91*, 4878–4881.
Harte, W. E., Jr., Swaminathan, S., Mansuri, M. M., Martin, J. C., Rosenberg, I. E., & Beveridge, D. L. (1990) *Proc. Natl. Acad. Sci. U.S.A. 87*, 8864–8868.
Jorgensen, W. L., & Tirado-Rives, J. (1989) *Chem. Scr. 29 A*, 191–196.
Kline, A. D., & Justice, R. M. (1990) *Biochemistry 29*, 2906–2913.
Kristensen, S. M., Jorgensen, A. M. M., Led, J. J., Balschmidt, P., & Hansen, F. B. (1991) *J. Mol. Biol. 218*, 221–231.
Krüger, P., Strassburger, W., Wollmer, A., & van Gunsteren, W. F. (1985) *Eur. Biophys. J. 13*, 77–88.
Krüger, P., Strassburger, W., Wollmer, A., van Gunsteren, W. F., & Dodson, G. G. (1987) *Eur. Biophys. J. 14*, 449–459.
Levitt, M., & Sharon, R. (1988) *Proc. Natl. Acad. Sci. U.S.A. 85*, 7557–7561.
Liang, D. C., Stuart, D., Dai, G. B., Todd, R., Iou, G. M., & Lou, M. Z. (1985) *Scienta Sinica 5*, 428–437.
Melberg, S. G., & Johnson, W. C. (1990) *Proteins 8*, 280–286.
Pocker, Y., & Biswas, S. B. (1980) *Biochemistry 19*, 5043–5049.
Roy, M., Lee, R. W. K., Brange, J., & Dunn, M. F. (1990) *J. Biol. Chem. 265*, 5448–5452.
Ryckaert, J.-P., Ciccotti, G., & Berendsen, H. J. C. (1977) *J. Comput. Phys. 23*, 327–341.
Shi Yun-yu, Yun Ru-huai, & van Gunsteren, W. F. (1988) *J. Mol. Biol. 200*, 571–577.
Van Belle, D., Prêvost, M., & Wodak, S. J. (1989) *Chem. Scr. 29 A*, 181–189.
van Gunsteren, W. F., & Berendsen, H. J. C. (1984) *J. Mol. Biol. 176*, 559–654.
van Gunsteren, W. F., & Berendsen, H. J. C. (1987) *Groningen Molecular Simulation* (GROMOS) *Library Manual*, Biomos, Nijenborgh 16, 9747 AG Groningen, The Netherlands.
van Gunsteren, W. F., & Berendsen, H. J. C. (1977) *Mol. Phys. 34*, 1311–1327.
Wodak, S. J., Alard, P., Delhaise, P., & Renneboog-Squilbin, C. (1984) *J. Mol. Biol. 181*, 317–322.
Wong, C. F., & McCammon, J. A. (1986a) *J. Am. Chem. Soc. 108*, 3830–3832.
Wong, C. F., & McCammon, J. A. (1986b) *Isr. J. Chem. 27*, 211–215.

NMR Study of the Phosphate-Binding Elements of *Escherichia coli* Elongation Factor Tu Catalytic Domain†

David F. Lowry,‡ Robbert H. Cool,§ Alfred G. Redfield,*,‡ and Andrea Parmeggiani§
Departments of Biochemistry and Physics, Brandeis University, Waltham, Massachusetts 02254, and Laboratoire de Biochimie, Ecole Polytechnique, SDI 61480 du Centre National de la Recherche Scientfique, F-91128 Palaiseau Cedex, France
Received June 21, 1991; Revised Manuscript Received August 29, 1991

ABSTRACT: The phosphoryl-binding elements in the GDP-binding domain of elongation factor Tu were studied by heteronuclear proton observe methods. Five proton resonances were found below 10.5 ppm. Two of these were assigned to the amide groups of Lys 24 and Gly 83. These are conserved residues in each of the consensus sequences. Their uncharacteristic downfield proton shifts are attributed to strong hydrogen bonds to phosphate oxygens as for resonances in N-ras-p21 [Redfield, A. G., & Papastavros, M. Z. (1990) *Biochemistry 29*, 3509–3514]. The Lys 24 of the EF-Tu G-domain has nearly the same proton and nitrogen shifts as the corresponding Lys 16 in p21. These results suggest that this conserved lysine has a similar structural role in proteins in this class. The tentative Gly 83 resonance has no spectral analogue in p21. A mutant protein with His 84 changed to glycine was fully ^{15}N-labeled and the proton resonance assigned to Gly 83 shifted downfield by 0.3 ppm, thereby supporting the assignment.

We are interested in the large class of purine nucleoside binding proteins that couple the binding and hydrolysis of purine triphosphate to some other useful function. Proteins of this class give rise to diverse processes such as polypeptide chain elongation and initiation, control of cell proliferation, muscle contraction, neurotransmission, and hormone action. These proteins appear similar in the way they bind purine triphosphate. They have one concensus element (henceforth element 1) Gly-X-X-X-X-Gly-Lys-(Ser or Thr), where X indicates a variable residue and parentheses indicate the possible residues of a single position that is not strictly conserved. Structural studies have shown that some of the amide protons in this element are pointing toward phosphate oxygens. The lysine side chain spans the element and the ε-amino group hydrogen bonds to the carbonyl group of the first glycine in

† Partially supported by USPHS Grant GM20168 to A.G.R. and by Grant ST2J-0388-C of the European Economical Community to A.P.
* To whom correspondence should be addressed.
‡ Brandeis University.
§ Ecole Polytechnique, CNRS.

0006-2960/91/0430-10872$02.50/0